

Multimodal Approach to Seismic Pavement Testing

Nils Ryden¹; Choon B. Park²; Peter Ulriksen³; and Richard D. Miller⁴

Abstract: A multimodal approach to nondestructive seismic pavement testing is described. The presented approach is based on multichannel analysis of all types of seismic waves propagating along the surface of the pavement. The multichannel data acquisition method is replaced by multichannel simulation with one receiver. This method uses only one accelerometer-receiver and a light hammer-source, to generate a synthetic receiver array. This data acquisition technique is made possible through careful triggering of the source and results in such simplification of the technique that it is made generally available. Multiple dispersion curves are automatically and objectively extracted using the multichannel analysis of surface waves processing scheme, which is described. Resulting dispersion curves in the high frequency range match with theoretical Lamb waves in a free plate. At lower frequencies there are several branches of dispersion curves corresponding to the lower layers of different stiffness in the pavement system. The observed behavior of multimodal dispersion curves is in agreement with theory, which has been validated through both numerical modeling and the transfer matrix method, by solving for complex wave numbers.

DOI: 10.1061/(ASCE)1090-0241(2004)130:6(636)

CE Database subject headings: Seismic tests; Nondestructive tests; Surface waves; Rayleigh waves; Pavements; Dispersion.

Introduction

Mechanistic and analytical models are the basis of modern pavement design. A prerequisite for using these models is that material properties, such as Young's modulus (E -modulus) and Poisson's ratio (ν), can be measured and validated in the field. Seismic nondestructive testing of pavements is of particular interest because of its ability to measure fundamental low strain physical properties, i.e., seismic velocities, by affecting a representative volume of the material in a nondestructive manner. Surface wave testing utilizes the dispersive nature of surface waves in a layered medium to evaluate elastic stiffness properties of the different layers. The complete procedure can be divided into three phases: (1) data collection at the surface; (2) evaluation of the experimental dispersion curve; and (3) evaluation of the shear wave velocity (V_s) with depth profile from the experimental dispersion curve, i.e., inversion.

The most established surface wave approach, the spectral analysis of surface wave (SASW) method (Heisey et al. 1982), is based on evaluation of phase velocity measurements between two receivers. This method is faster than the earlier steady state ap-

proach (Van der Pol 1951), with the limitation that only one phase velocity can be evaluated at each frequency. SASW measurements have been continuously enhanced and have proved to be useful for pavement testing (Nazarian 1984; Aouad 1993; Nazarian et al. 1999). However, several writers have reported on limitations and difficulties related to surface wave measurements based on the two-receiver approach, especially at pavement sites. Most of these difficulties are reported to originate from the influence of higher modes of propagation (Hiltunen and Woods 1990; Rix et al. 1991; Al-Hunaidi 1992; Tokimatsu et al. 1992; Stokoe et al. 1994; Al-Hunaidi and Rainer 1995; Ganji et al. 1998; Ryden 1999). Several researchers have also proposed on a variety of alternatives to handle the influence of higher modes (Sanchez-Salinerio et al. 1987; Gucunski and Woods 1992; Al-Hunaidi 1998; Ganji et al. 1998; Gucunski et al. 2000). All these proposed alternatives improved the overall performance of the seismic surface wave testing method based on the two-receiver approach. However, the limitation remains that only one phase velocity can be evaluated at each frequency. The SASW method cannot separate different modes of propagation over a pavement system and thus measures a superposition of all propagating waves at the specific receiver locations. This superposed effect, often termed apparent phase velocity or pseudophase velocity, changes with offset (distance) (Zywicki 1999) and has forced the evaluation of the data to take into account the position of the receivers and the superposition of different modes for the inversion of experimental dispersion curves. An alternative procedure, so far only performed at soil sites, is to delineate different modes of propagation in the measurements, and use theoretically calculated multiple mode dispersion curves for the inversion (Xia et al. 2000; Valentina et al. 2002).

It is the aim of this paper to propose a new approach in seismic pavement testing where the different modes of propagation are separated, thereby potentially clarifying some of the noted difficulties with the SASW method applied to pavement testing. This new approach is based on the multichannel analysis of surface wave (MASW) data processing technique (Park et al. 1998, 1999;

¹Graduate Student, Dept. of Engineering Geology, Lund Univ., P. O. Box 118, SE-22100 Lund, Sweden. E-mail: nils.ryden@tg.lth.se

²Assistant Scientist, Geophysics, Kansas Geological Survey, Univ. of Kansas, 1930 Constant Avenue, Lawrence, KS 66047-3726. E-mail: park@kgs.ku.edu

³Associate Professor, Dept. of Engineering Geology, Lund Univ., P. O. Box 118, SE-22100 Lund, Sweden. E-mail: peter.ulriksen@tg.lth.se

⁴Associate Scientist, Geophysics, Section Chief, Kansas Geological Survey, Univ. of Kansas, 1930 Constant Avenue, Lawrence, KS 66047-3726. E-mail: rmiller@kgs.ku.edu

Note. Discussion open until November 1, 2004. Separate discussions must be submitted for individual papers. To extend the closing date by one month, a written request must be filed with the ASCE Managing Editor. The manuscript for this paper was submitted for review and possible publication on August 24, 2001; approved on August 6, 2003. This paper is part of the *Journal of Geotechnical and Geoenvironmental Engineering*, Vol. 130, No. 6, June 1, 2004. ©ASCE, ISSN 1090-0241/2004/6-636-645/\$18.00.

2001), and the multichannel simulation with one receiver (MSOR) method (Ryden et al. 2001) of data acquisition. The nature of multimode dispersion curves in a pavement system is first studied from a theoretical point of view. Key aspects of the field procedure MSOR and the MASW processing technique are presented to describe how multimode dispersion curves can be extracted from multichannel data. Finally the proposed approach is described along with a case study.

Wave Propagation in Pavement Systems

In surface wave testing of pavements, the experimental dispersion curve is often interpreted to represent Rayleigh waves. However, free Rayleigh waves can only propagate at phase velocities slower than the shear wave velocity of the half-space (Thrower 1965). Phase velocities violating this condition are leaking modes and are not free surface waves (Buchen and Ben-Hador 1996). These leaking modes are all guided plate waves formed by the superposition of reflected compression (P) and shear (S) waves within each layer. Thus, the Rayleigh wave is only one of several types of guided dispersive waves propagating in a pavement structure that may be measured at the surface and used for material characterization.

Early work with the steady state method applied to pavements showed that measured phase velocities in the high frequency range corresponds to the fundamental mode of antisymmetric (A_0) Lamb wave propagation in a free plate (Jones 1955; Vidale 1964; Jones and Thrower 1965). Martincek (1994) verified that the Lamb wave solution was valid from the shortest measurable wavelengths up to wavelengths of six to seven times the thickness of the top layer. Early studies also reported on more than one phase velocity propagating at certain frequencies (Van der Pol 1951; Jones 1955; Heukelom and Foster 1960), thereby indicating the presence of higher modes of propagation. In the work by Jones (1962) and Vidale (1964) it was theoretically revealed that dispersion curves from pavement sites are not continuous with frequency or wavelength, also pointed out by Yuan and Nazarian (1993). Vidale (1964) concluded that there exist as many branches of dispersion curves as there are layers in the construction.

In the case of a free plate, Lamb (1917) derived a dispersion equation where the quasi-longitudinal wave (longitudinal wave in plates), the bending wave, and the Rayleigh wave are all included, termed free Lamb waves. Free Lamb waves propagating in the plane of a free plate are only possible for certain combinations of frequency (f) and phase velocity (c) corresponding to standing waves in the thickness (h) direction. Possible combinations are given by the dispersion relation:

$$\frac{\tan\left(\beta \frac{h}{2}\right)}{\tan\left(\alpha \frac{h}{2}\right)} = - \left[\frac{4\alpha\beta k^2}{(k^2 - \beta^2)^2} \right]^{\pm 1} \quad (1)$$

where

$$\alpha^2 = \frac{\omega^2}{V_P^2} - k^2 \quad (2)$$

$$\beta^2 = \frac{\omega^2}{V_S^2} - k^2 \quad (3)$$

The \pm sign on the right-hand term of Eq. (1) represents, symmetric (+), and antisymmetric (-), type of wave propagation with respect to the midplane of the plate, see Fig. 1(b). Material stiff-

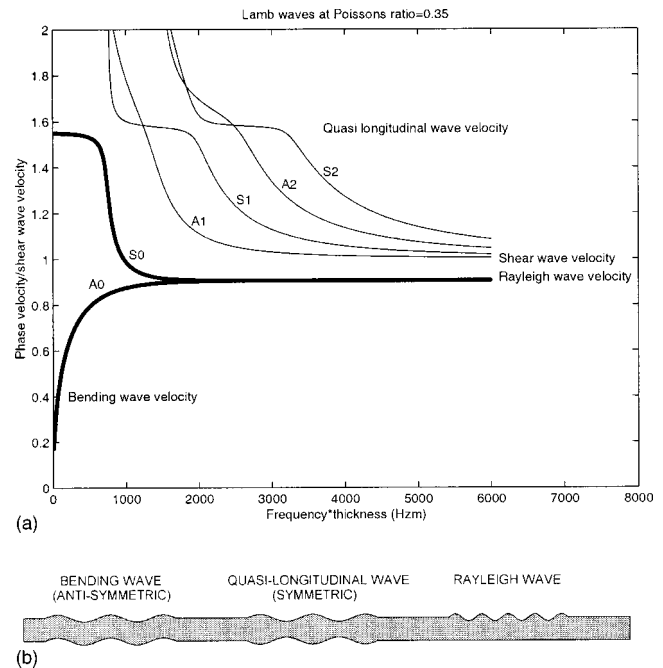


Fig. 1. (a) Lamb wave dispersion curves in free plate. In (b), particle motion is illustrated for pure form of different type of Lamb waves.

ness properties are given by V_S and V_P . Using the angular frequency ($\omega = 2\pi f$), and the wave number ($k = \omega/c$), a root searching technique has to be used to calculate dispersion curves for a given plate (Graff 1975). In Fig. 1(a) the symmetrical and antisymmetrical modes of wave propagation has been derived from Eq. (1) with a V_S/V_P ratio corresponding to a Poisson's ratio of 0.35, given by

$$\nu = \frac{0.5(V_P/V_S)^2 - 1}{(V_P/V_S)^2 - 1} \quad (4)$$

It should be noted that the phase velocity and frequency axes can be normalized with respect to the shear wave velocity and the thickness of the plate for a given Poisson's ratio. The different types of wave propagation are indicated on the dispersion curves and the fundamental mode particle motion is indicated on the plate below the dispersion curves [Fig. 1(b)]. Higher modes of symmetrical and antisymmetrical wave motion develop at their respective cutoff frequency (Graff 1975), which is related to the plate thickness.

The theory given above is only valid for a free plate. However as stated above several researchers have reported that the Lamb wave solution of the top layer only, is valid for a layered pavement up to wavelengths of six to seven times the thickness of the top layer. Theoretical dispersion curves for a layered elastic medium are usually calculated with a matrix formulation based on wave propagation theory. The most widely used formulation is the transfer matrix method (Thomson 1950; Haskell 1953). The derivation of the problem and some aspects on numerical implementations are discussed in the literature (Thrower 1965; Dunkin 1965; Kausel and Roesset 1981; Lowe 1995) and are thus omitted here. The wave number that makes the value of the determinant of the global matrix (assembled from all layer matrixes) vanish is searched for each frequency. Generally only the real part of the wave number (k_r) that makes the real part of the determinant vanish is solved in the traditional SASW inversion procedure (Stokoe et al. 1994).

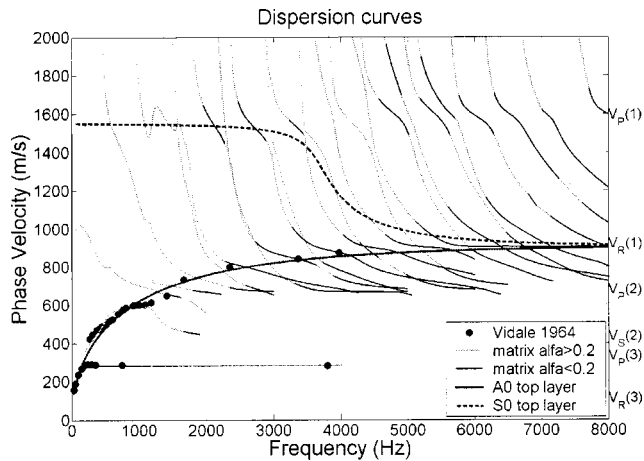


Fig. 2. Theoretical dispersion curves derived from transfer matrix method by solving for both real and complex part of wave number. Fundamental modes of Lamb waves for free plate with properties as of top layer (from Table 1) are plotted with thicker solid and dotted lines.

In pavement structures the wave number is only purely real at phase velocities slower than the shear wave velocity of the half-space, representing free Rayleigh wave propagation. At higher phase velocities the wave number contains a small imaginary part (k_j), representing leaky modes. The ratio α given by

$$\alpha = \frac{2\pi k_j}{k_r} \quad (5)$$

represents an extra attenuation factor unique for systems where the velocity decreases with depth or for a plate in water (Vidale 1964). Modes with a small imaginary part of the wave number are termed leaky modes because energy is radiated to the coupling medium in proportion to α (Lowe 1995). Solving for both the real and the imaginary part of the wave number is computationally demanding but cannot be ignored when theoretical dispersion curves for pavement systems are calculated.

In Fig. 2 dispersion curves have been calculated from the layer model in Table 1 by solving for both the real and the imaginary part of the wave number. A theoretical pavement structure studied by Vidale (1964) has been used for comparison purposes (see Table 1). Black lines represent poles where $\alpha < 0.2$ and gray lines represent poles where $\alpha > 0.2$. As α increases, the wave changes from propagating to oscillatory motion. The points calculated by Vidale (1964) using a different matrix formulation are presented as solid circles in Fig. 2. It is shown that there exist many different modes of dispersion curves. As indicated in Fig. 2, there are several asymptotic trends of phase velocities corresponding to seismic velocities in the theoretical layer model (Table 1). The fundamental modes of symmetrical (S0) and antisymmetrical (A0) free Lamb waves are plotted as dotted and solid thicker lines to illustrate how higher modes with lower attenuation (α

< 0.2) follow the trend of Lamb waves. The number of modes increases with frequency and the complexity of finding and calculating all modes can become large. A complete description of this procedure is not possible within this paper and will be addressed in future publications.

Multichannel Recording and its Simulation

The multichannel method, in general, aims at a maximized discrimination of signal against various types of noise based on unique two-dimensional (2D) patterns of seismic waves in time-offset ($t-x$), frequency-offset ($f-x$), or frequency-wave number ($f-k$) domain (Yilmaz 1987). True multichannel data acquisition deploys multiple receivers placed on top of a medium surface with an equal spacing along a linear survey line. Each receiver is connected to a common multichannel recording instrument (seismograph) where a separate channel is dedicated to recording signals from each receiver. The multichannel method is a pattern-recognition method that can delineate the complexity of seismic characteristics through the coherency measurement in velocity and attenuation of different types of seismic waves (e.g., multimodal surface waves, various types of body waves, and a wide range of ambient noise). In addition to this advantage in the effectiveness of signal extraction, it also provides a redundancy in measurement through the field procedure.

A true multichannel survey requires an expensive and bulky multichannel (e.g., 48-channel) recording device and many receivers deployed simultaneously in a small area. However, in seismic pavement testing, where the survey dimension is microscopic in comparison to the conventional exploration survey, this would indicate a formidable survey expense and also an inconvenient field procedure with many components and complicated wiring deployed in a small area. Instead, the multichannel recording can be simulated with only one receiver and a single-channel recording device: multichannel simulation with one receiver (MSOR) (Ryden et al. 2001). There are two alternative approaches to this simulation. One is to fix the source point and move the receiver point consecutively by the same amount of distance along a preset survey line after obtaining a single-channel measurement at one point. The other approach is to fix the receiver point and move the source point in the same way [Fig. 3(a)]. Then a simulated multichannel record is constructed by compiling all individual seismic traces in the acquired order. In any case, a horizontally traveling seismic wave will appear on the record with its arrival pattern following a linear trend whose slope gives the velocity of the wave [Fig. 3(b)]. Either of these two alternatives will give a result identical to that obtained through the true multichannel method provided the following conditions are met:

1. There is no significant lateral change in the thickness of each layer that is assumed to be homogeneous within the surveyed distance; and
2. There is no significant inconsistency in triggering.

Table 1. Theoretical Pavement Profile Representing Case EB12 Studied by Vidale (1964)

Layer	Thickness (m)	Poisson's ratio	Density (kg/m ³)	V_S (m/s)	V_P (m/s)	V_R (m/s)
1	0.2	0.167	2000	1000	1581	906
2	0.4	0.167	2000	419	663	378
3	∞ (matrix)	0.450	2000	96	318	91

15.4 (fast Lagrangian analysis of continua)

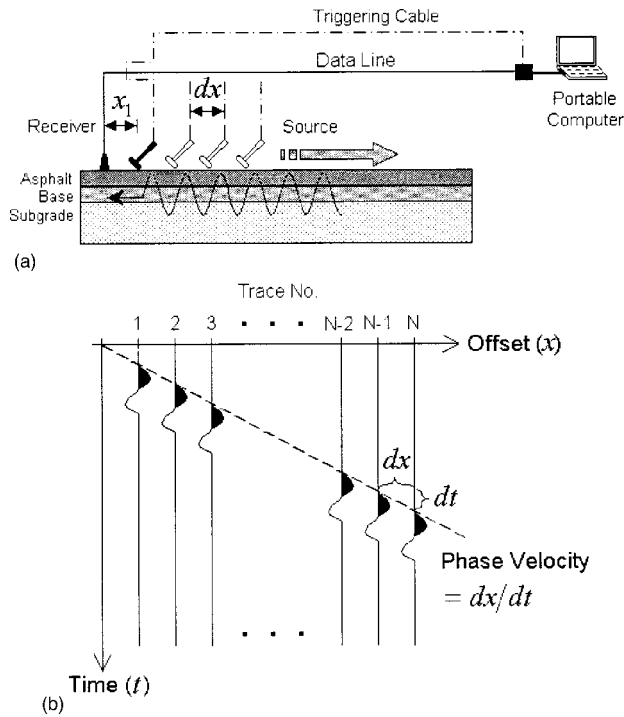


Fig. 3. (a) Schematics illustrating multichannel simulation with one receiver survey with fixed receiver and moving source. In (b), true (or simulated) multichannel record is schematically illustrated.

In practice, the first assumption is usually met to a sufficient extent in pavement testing, and the second is related to the precision of the triggering mechanism. The latter can be readily noticed once a compiled record is displayed, and in addition, a remedial processing technique is available to compensate for the inconsistency to a certain degree (Park et al. 2002). Considering a greater difficulty in ensuring a satisfactory coupling between receiver and medium surface in the case of the receiver-moving approach, the source-moving approach is utilized in this study. A simulated multichannel record is referred to as an MSOR record, or simply a record.

In this study, the data acquisition system was triggered with an accelerometer attached on the impact source. By using a comparator circuit the system is triggered at a preselected level of the accelerometer signal. Only one high frequency source, a 0.22 kg carpenter hammer, has been used to cover all frequencies of interest. To improve source coupling and the precision of the source point, a steel spike has been used as a source-coupling device. An accelerometer with a natural resonance frequency of 30 kHz was used as the receiver and was attached to the pavement with sticky grease.

The data acquisition system consists of a portable computer equipped with a PC-card, source, receiver, and external signal conditioning. This configuration is called the portable seismic acquisition system (PSAS) (Ryden et al. 2002). A PC-card from Measurement Computing, Middleboro, Mass. (PC-CARD DAS-16/16-AO), has been used. This card has a single-channel sample rate of 200 kSa/s with a 16-bit dynamic range. With the PSAS system the MSOR method is implemented efficiently because data are streamed directly to the computer and all impacts can be generated with intervals only fractions of a second apart. The PSAS system was developed at the department of Geotechnology, Lund University, and is further described in Ryden et al. (2002).

Phase Velocity Analysis Scheme

Here, the dispersion analysis scheme as normally adopted in the MASW method is described. More detailed description can be found in Park et al. (1998; 2001). A N -channel record mr_N is defined as an array of N traces collected by one of the aforementioned acquisition methods: $mr_N = r_i$ ($i = 1, 2, \dots, N$) with its frequency-domain representation of $MR_N(\omega) = R_i(\omega) = FFT[r_i]$ ($i = 1, 2, \dots, N$). Then, $R_i(\omega)$ can be written as a product of amplitude, $A_i(\omega)$, and phase, $P_i(\omega)$, terms: $R_i(\omega) = A_i(\omega)P_i(\omega)$. $A_i(\omega)$ changes with both offset (i) and angular frequency (ω) due to spherical divergence, attenuation, and the source spectrum characteristics. $P_i(\omega)$ is the term that is determined by phase velocity (c) of each frequency

$$P_i(\omega) = e^{-j\Phi_i(\omega)} \quad (6)$$

where

$$\Phi_i(\omega) = \omega x_i / c = \omega \{x_1 + (i-1)dx\} / c \quad (7)$$

Consider one specific frequency (e.g., 10 kHz) of $R_i(\omega)$. Its time-domain representation will be an array of sinusoid curves of the same angular frequency, but with different amplitude and phase. Since the amplitude does not contain any information linked to phase velocity, $R_i(\omega)$ can be normalized without loss of significant information

$$R_{i,\text{norm}}(\omega) = R_i(\omega) / |R_i(\omega)| = P_i(\omega) \quad (8)$$

Fig. 4(a) shows an array of normalized sinusoid curves for an arbitrary frequency of 10 kHz propagating at another arbitrary phase velocity of 1,420 m/s. Sinusoid curves in the figure have the same phase along a slope (S_0) of the phase velocity, whereas they have a different phase along the slopes of other phase velocities, as indicated in the figure. Therefore, if the curves are summed together within a finite time length (e.g., one period) along the slope S_0 , then it will give another sinusoid curve of finite length whose amplitude (A_S) is N . On the other hand, A_S will be smaller than N if the summation is performed along other slopes. This principle is the key element of the dispersion analysis employed in the MASW method. In practice the summation can be performed in a scanning manner along many different slopes specified by different phase velocities changing by small increments (e.g., 5 m/s) within a given range (e.g., 100–5,000 m/s). The result of each summation as represented by amplitude (A_S) of summed sinusoid curves can be then displayed in a 2D format (i.e., phase velocity versus A_S). In this 2D scanned curve, the phase velocity that gives the maximum amplitude ($A_{S,\text{max}}$) will be the correct value being sought [Fig. 4(b)]. As illustrated in Fig. 4(b), the 2D scanned curve has one main lobe with a peak amplitude $A_{S,\text{max}}$ and many side lobes on both sides. It is the sharpness of this main lobe that affects the resolution and accuracy of the analyzed dispersion relationship. In Park et al. (2001) a detailed parametric examination of the scanning method on its resolution in response to change in such parameters as N , c , dx , and ω is presented. Generally the sharpness of the peak A_S increases with N , and this means that more traces will ensure higher resolution in the determination of a phase velocity. This effect is illustrated in Fig. 4(b) for N values of 2, 20, and 80 traces. A_S has been normalized with respect to N so that the peak value is one in all three cases.

The aforementioned summation operation can actually be accomplished in the frequency domain

$$A_S(c_T) = e^{-j\delta_{1,T}} R_{1,\text{norm}}(\omega) + e^{-j\delta_{2,T}} R_{2,\text{norm}}(\omega) + \dots + e^{-j\delta_{N,T}} R_{N,\text{norm}}(\omega) \quad (9)$$

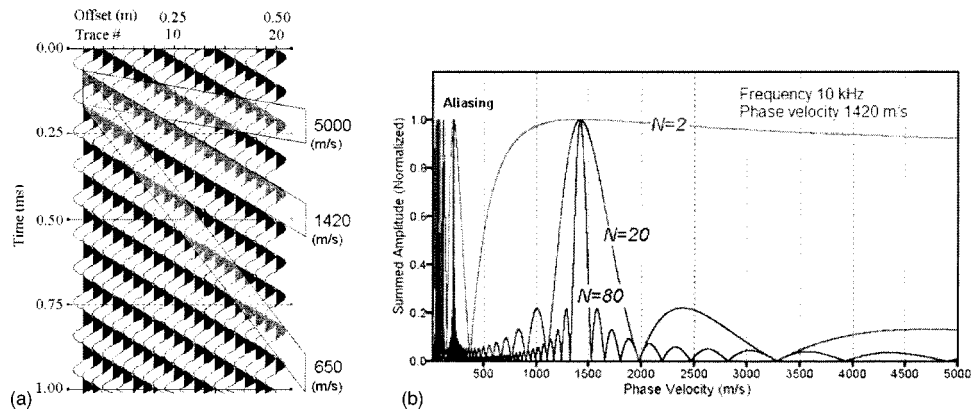


Fig. 4. (a) Synthetic record where single-frequency (10 kHz) component of seismic wave is displayed with phase velocity of 1,420 m/s, and (b) corresponding summed amplitude curves for different number of traces (N).

where

$$\delta_{i,T} = \omega \left[\{x_1 + (i-1)dx\} / c_T \right] \quad (10)$$

This is a phase term that increases with offset (distance) (x) and determined by a testing phase velocity (c_T) within a scanning range. $A_S(c_T)$ is a complex number whose absolute value ($|A_S(c_T)|$) is the same as the amplitude (A_S) of summed sinusoid wave in time domain previously explained.

When seismic wave propagation invokes multimodal characteristics (like inclusion of higher modes) or includes different types of waves (like body and surface waves together), a multiple number of phase velocities can exist at the same frequency. This multiphase-velocity case can be treated as a linear superposition of individual single-phase-velocity cases. For example, if there exists a fundamental mode ($M0$) [Fig. 5(a)] and one higher mode ($M1$) [Fig. 5(b)] at the same frequency with different phase velocities and amplitudes, the measured wavefield then would be the same as a superposition [Fig. 5(c)] of the two separate records [Figs. 5(a) and (b)]. This means that if the phase-velocity scanning is applied to this multimodal record, the resulting scanned curve will be the same as a superposition [Fig. 5(e)] of the two individual scanned curves [Fig. 5(d)] obtained from each single-mode record. Park et al. (2001) shows that in this case, however, the superposition involves a scaling term determined by the relative energy partitioning between the two modes. Therefore, two main lobes appear with different peak amplitudes. This is additional information that would be critical for the study of energy partitioning between different modes or different types of seismic waves along the survey line. To identify dispersion curves, all 2D curves at different frequencies are assembled to a 3D image showing the energy distribution as a function of phase velocity and frequency. This is illustrated with a numerical modeling example in the next section.

Numerical Test

A numerical example is presented to show that the phase velocity analysis scheme can delineate multiple wave propagation modes in pavements. For comparison purposes we study the same theoretical layer model presented earlier and used by Vidale (1964) (Table 1).

The computer code FLAC (fast Lagrangian analysis of continua) (Itasca 2000) has been used in the numerical study. FLAC is a commercially available 2D explicit finite difference code. The

program utilizes a time-marching method to solve the equation of motion. The nature of the problem was assumed to be axisymmetric with a linear elastic material model; i.e., no material damping was introduced. The upper horizontal axis of the model is free of any constraint so that surface waves can develop along the surface. The horizontal bottom and right side of the model has viscous boundary conditions in order to absorb as much energy as possible, thereby minimizing reflections from the edges. A finite difference mesh of cells (800×800) was set up. Internally FLAC divides each cell into four triangular subcells (Itasca 2000). Cell size (0.005×0.005 m) was set up following recommendations by Kuhlemeyer and Lysmer (1973). They showed that for accurate modeling of wave propagation the cell size should be ten times smaller than the wavelength modeled. A Ricker wavelet was applied as a velocity history in the upper left corner of the model (at zero offset). The Ricker wavelet had a 100% bandwidth and a 700 Hz center frequency. The pulse is truncated where the envelope falls 60 dB below the peak amplitude. Time step (5 μs) was set up according to the recommendations of Zerwer et al. (2002).

Vertical acceleration histories on the surface at incremental offsets (0–8 m) from the source were extracted from the FLAC model. These histories were combined into a multichannel record as normally results from MSOR measurements. When this record is analyzed by the scanning method and the scanned results are displayed in a 3D format, the pattern of main lobes creates a gray scale image of dispersion curves (Fig. 6). This type of display will be informative for identifying different modes (or types) of seismic waves.

There are several branches of dispersion curves visible in Fig. 6. As expected, almost all branches and modes of dispersion curves match with dispersion curves derived with the matrix formulation (solving for complex wave numbers) (compare Fig. 6 with Fig. 2). This theoretically confirms the ability of the presented phase velocity analysis scheme to delineate multiple dispersion curves from a pavement site, provided a multichannel record has been measured or simulated with the MSOR technique. Dispersion curves corresponding to free Lamb waves calculated from the properties of the top layer only are also plotted in the dispersion curve image. This illustrates how the overall trend of all branches follow the A0 Lamb wave dispersion curve of the top layer only. It should also be noted that the image of dispersion curves is obtained automatically and objectively from the multichannel record without going through any filtering of

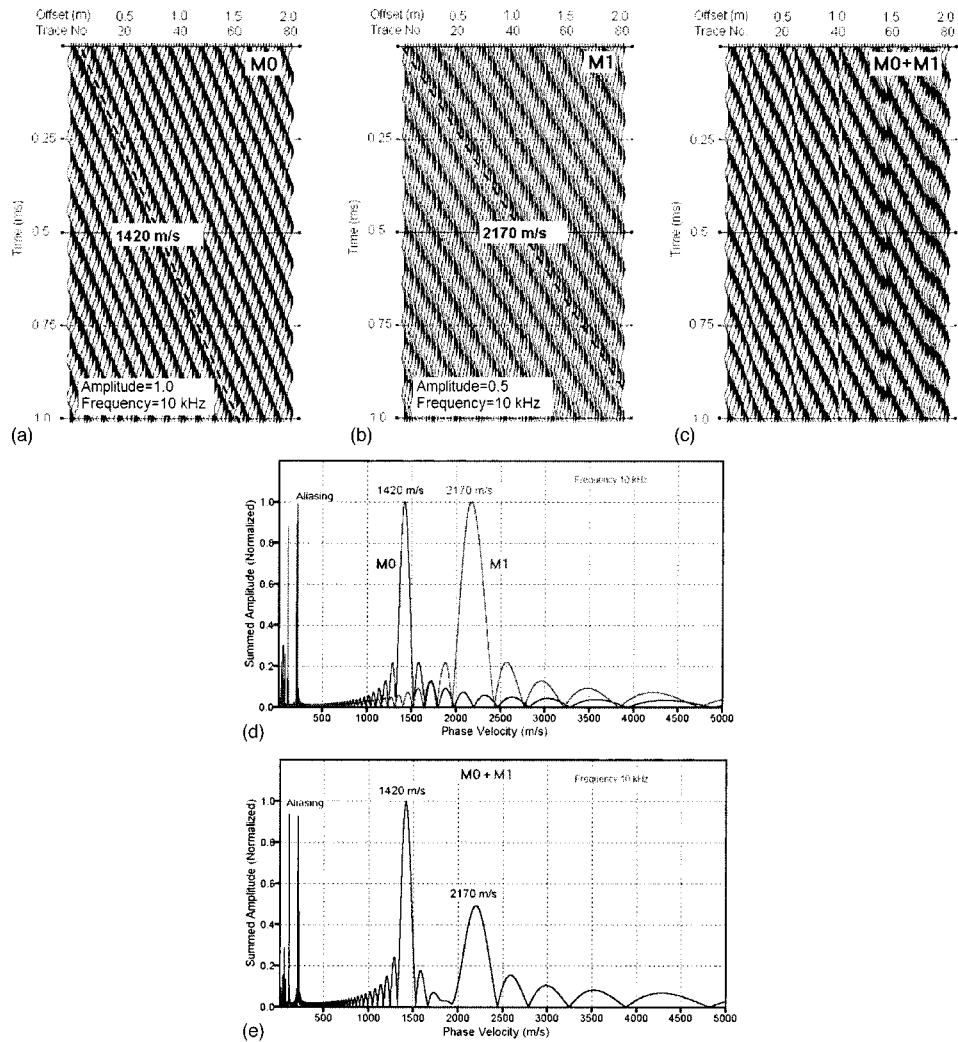


Fig. 5. Synthetic records that model single-frequency (10 kHz) component (a) of fundamental mode (M_0) with phase velocity of 1,420 m/s, (b) of higher mode (M_1) with phase velocity of 2,170 m/s and with a relative energy only half that of fundamental mode, and (c) of both modes (M_0 and M_1) propagating simultaneously. Phase velocity scanning curves obtained from records in (a) and (b) are displayed in (d) and same curve obtained from the multimodal record of (c) is displayed in (e).

near and far field effects and without problems of phase unwrapping.

Field Test

MSOR measurements were conducted at the Denmark Technical University (DTU) at the testing facility for the Danish Road Testing Machine. Several full-scale pavement constructions have been built and tested here in an enclosed climate controlled chamber (Zhang and Macdonald 2001). The complete pavement construction inside the testing facility is 20 m long, 2.5 m wide, and 2 m thick. This test site was chosen to obtain the best possible controlled environment where temperature and layering are well defined. The given layering at the DTU test site is presented in Table 2.

Following the MSOR method, one accelerometer was located at zero offset. The PSAS was set to 200 kHz sample rate. While keeping the accelerometer at zero offset and by changing the impact points of the hammer from offset 0.025 to 2.0 m with 0.025 m impact separation, data were collected with 40 ms record

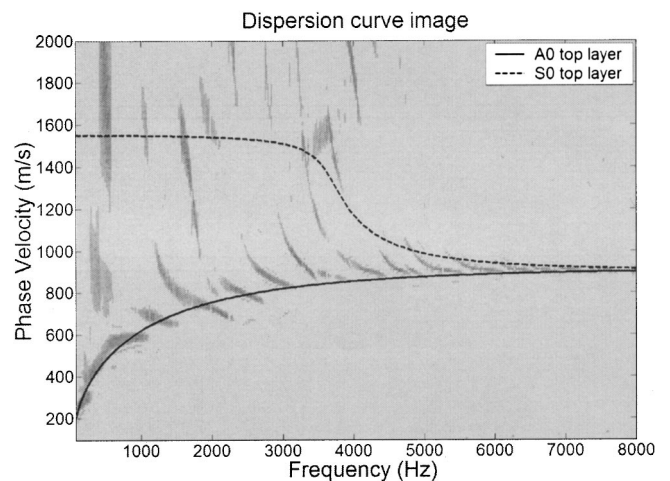


Fig. 6. Frequency-phase velocity image, created from presented phase velocity analysis scheme and synthetic data obtained from numerical modeling of pavement profile in Table 1

Table 2. Layering at Denmark Technical University Test Site

Layer	Thickness (m)
Asphalt 1 (high porosity)	0.036
Asphalt 2 (low porosity)	0.084
Base (granular material)	0.140
Subgrade (clay till)	1.376
Drainage layer (sand)	0.181
Concrete	0.250
Natural soil	~10.000

length using the equipment described earlier. At each offset five impacts were made with the spike kept in a fixed position. The asphalt temperature was 20°C.

The resulting multichannel record in offset-time domain is presented in Fig. 7. Each trace represents a stack of the last four signals from each impact point (offset). The first stroke at each impact point is only used to stabilize the source point. The main wave fronts seen in Fig. 7 are low frequency (about 1 kHz) surface waves. Fig. 8 shows the corresponding amplitude spectrum of the complete multichannel record. Beyond 0.7 m offset there is no significant energy at high frequencies (>5 kHz).

As an intermediate step toward the transformation to the 3D frequency-phase velocity image, the multichannel record in Fig. 7 is plotted in single frequency format at 5,800 Hz [Fig. 9(a)]. At this frequency two main patterns (phase velocities) can be identified, indicated with straight lines in the figure. From the offset (horizontal axis) and the time (vertical axis) the phase velocity of each line (pattern) is calculated to 1,338 and 2,705 m/s, respectively. It should be observed that although the energy above 5 kHz is very low at far offsets (>0.7 m) in the amplitude spectrum presented in Fig. 8, there is still a coherent phase velocity pattern in Fig. 9(a) extending all the way to 2.0 m offset when the data is plotted in multichannel format. If there were only random noise in this frequency range at offsets larger than 0.7 m there should not be any coherency in the phase velocity pattern. Applying the presented phase velocity analysis scheme at the same frequency clearly identifies the two-phase velocities [Fig. 9(b)].

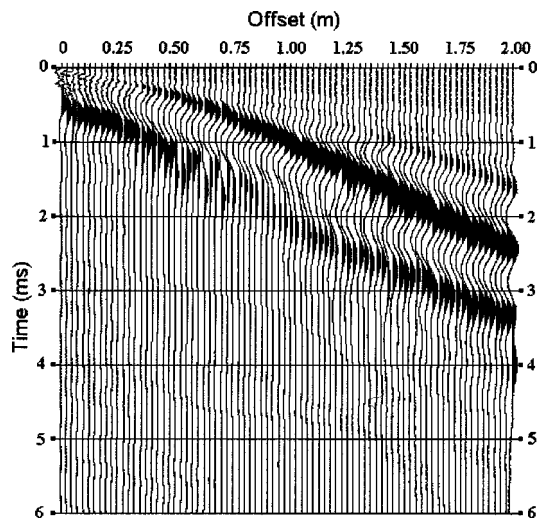


Fig. 7. Compiled multichannel record obtained from multichannel simulation with one receiver measurements at Denmark Technical University test site

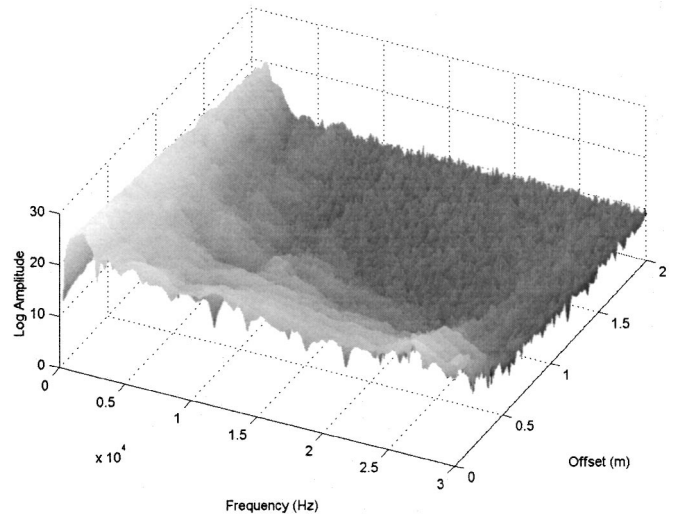


Fig. 8. 3D amplitude spectrum from recorded data at Denmark Technical University test site

In Fig. 10 the full record is automatically transformed to the frequency-phase velocity domain by using the presented phase velocity scheme of the MASW wavefield transformation method (Park et al. 1998, 2001). The phase velocity image shows phase velocity dispersion up to 28 kHz above which the surface waves are spatially aliased due to the distance between impact points.

In Fig. 10 the theoretical fundamental mode dispersion curves of antisymmetric (A_0) and symmetric (S_0) Lamb waves [Eq. (1)] are plotted on top of the phase velocity contour curves. An almost perfect match is obtained for the given thickness of 0.120 m (Table 2), with a Poisson's ratio of 0.35 and a shear wave velocity of 1,611 m/s. By assuming or measuring the bulk density (ρ), the low strain shear modulus (G) can be calculated using

$$G = \rho V_S^2 \quad (11)$$

and the low strain Young's modulus, E , can also be determined by using

$$E = 2G(1 + \nu) \quad (12)$$

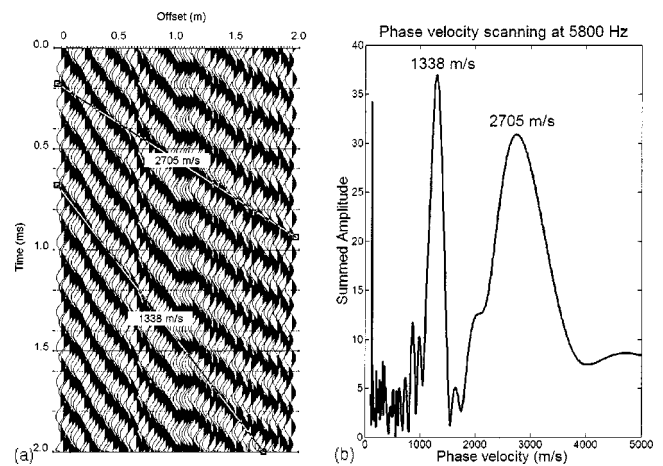


Fig. 9. (a) Single-frequency (5,800 Hz) display of data in Fig. 7 showing two different slopes (phase velocities) at same frequency. In (b), two velocities are identified as peaks in 2D scanned amplitude curve.

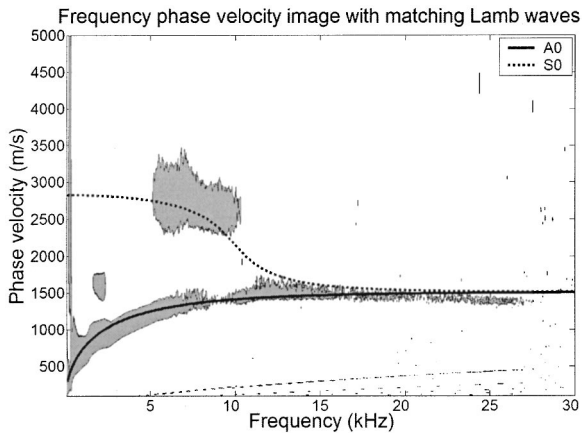


Fig. 10. Frequency-phase velocity image of Denmark Technical University data presented as contour plot at summed amplitude of 25 [compare with Fig. 9(b)]. Theoretical free Lamb wave dispersion curves have been matched to experimental data.

Setting the asphalt bulk density to $2,400 \text{ kg/m}^3$, the dynamic E modulus of the asphalt layer is calculated to 16.8 GPa. This modulus is only representative for the temperature and frequency during the measurement (i.e., 20°C and 15 kHz). The representative frequency 15 kHz is here taken from the part where the matching A0 dispersion curve is approaching a constant velocity.

At frequencies higher than 15 kHz the measured phase velocity is decreasing as in the case of normal Rayleigh wave dispersion where the velocity increases with depth. This can be explained from the higher porosity (lower stiffness) of the thin top asphalt layer (Table 2). To resolve the stiffness of this thin layer, frequencies higher than 28 kHz should have been measured.

In Fig. 11 the phase velocity image is plotted in a larger scale centered around 750 m/s and 1750 Hz, and is now presented with contour curves at a higher summed amplitude level. There are three different branches of dispersion curves visible in the image. Cutoff frequencies and abruptly changing phase velocities separate the branches. This correlates with the predicted theory presented by Vidale (1964), where each branch corresponds to each

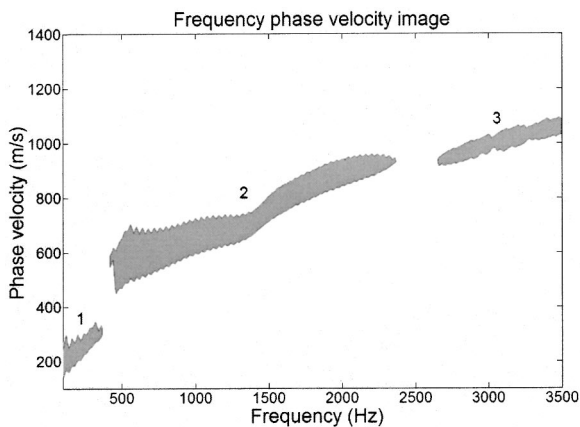


Fig. 11. Frequency-phase velocity image (contour curves at summed amplitude of 35) displayed in smaller frequency and phase velocity range

layer in the pavement. In Fig. 11 the different branches (i.e., layers), are marked 1 subgrade, 2 base, and 3 asphalt layer (start of the A0 mode).

Discussion

A multimodal approach to nondestructive seismic pavement testing has been described. In summary, the most critical factors for a successful simulation of a true multichannel shot gather on a pavement surface are (1) no significant lateral change in the thickness of each layer that is assumed to be homogeneous within the surveyed distance; (2) accurate triggering; and (3) minimized source-related discontinuities in waveform and statics.

Multiple dispersion curves are automatically and objectively extracted using the presented phase velocity analysis scheme of the MASW method. This processing scheme reduces the analysis time and the risk for operator-related errors in the conventional data reduction and phase unwrapping process. There is no need for any wavelength filter criteria or multiple sources to extract all frequencies of interest. The reported difficulties with extracting correct dispersion curves from phase velocity measurements between two receivers are thus avoided.

Resulting dispersion curves in the high frequency range match with theoretical Lamb waves in a free plate. At lower frequencies there are several branches of dispersion curves corresponding to each layer of different stiffness in the pavement system. The observed behavior of multimodal dispersion curves is in agreement with theory, which has been validated through both numerical modeling and the transfer matrix method, by solving for complex wave numbers. Results indicate that dispersion of stress waves in a pavement system cannot be represented with only one average dispersion curve. Especially at low frequencies (50–3,000 Hz) it seems necessary to resolve the different modes of dispersion curves to increase the overall resolution in seismic pavement testing.

At this stage stiffness properties and the thickness of the top pavement layer are evaluated by matching theoretical dispersion curves of symmetrical and antisymmetrical Lamb waves in a free plate. Several researchers have utilized this approach before, but only with the fundamental antisymmetrical mode (Jones 1955; Jones and Thrower 1965; Akhlaghi and Cogill 1994; Martincek 1994). It is believed that with the approach presented the identification of additional higher modes of dispersion curves will be possible, increasing the resolution of the final result.

To further investigate the possibility of a simplified approach for evaluating the stiffness properties of all layers in the pavement construction, we intend to study how measurable branches are related with the material properties of the layered medium, through the analytical matrix approach, numerical finite difference modeling, and field tests with the MSOR method. This is a critical step in the progression toward a refined and efficient seismic nondestructive testing technique for pavements.

Acknowledgments

The writers would like to give their sincere thanks to Peab Sverige AB, VINNOVA, and the Swedish road authority Vägverket, for financing this project, and to Professor Anders Bodare and Dr. Jonas Brunlid for help with the transfer matrix method, Professor Per Ullidtz for the opportunity to use the RTM facility at DTU, and Mary Brohammer for her assistance in the preparation of this manuscript.

Notation

The following symbols are used in this paper:

A = amplitude term;
 AO = fundamental mode of antisymmetric Lamb wave;
 c = phase velocity;
 dx = incremental distance between receiver or source stations;
 E = Young's modulus;
 f = frequency;
 h = thickness;
 k = wave number;
 MR = multichannel record in frequency domain;
 MO = fundamental mode;
 $M1$ = first higher mode;
 mr = multichannel record in time domain;
 N = number of channels;
 P = phase term;
 R = record in frequency domain;
 r = record in time domain;
 S = slope;
 SO = fundamental mode of symmetric Lamb wave;
 t = time;
 V_P = compression (longitudinal) wave velocity;
 V_R = Rayleigh wave velocity;
 V_S = shear (transverse) wave velocity;
 x = offset (distance between source and measurement point);
 α = attenuation factor;
 λ = wavelength;
 ν = Poisson's ratio;
 ρ = density; and
 ω = angular frequency.

Subscripts and Superscripts

a = average value;
 i = offset index (channel number);
 j = imaginary part;
 N = number of channels;
 r = real part;
 s = slope; and
 T = testing (phase velocity).

References

- Akhlaghi, B. T., and Cogill, W. H. (1994). "Application of the free plate analogy to a single-layered pavement system." *Insight*, 36(7), 514–518.
- Al-Hunaidi, M. O. (1992). "Difficulties with phase spectrum unwrapping in spectral analysis of surface waves nondestructive testing of pavements." *Can. Geotech. J.*, 29, 506–511.
- Al-Hunaidi, M. O. (1998). "Evolution-based genetic algorithms for analysis of non-destructive surface wave tests on pavements." *NDT & E Int.*, 31(4), 273–280.
- Al-Hunaidi, M. O., and Rainer, J. H. (1995). "Analysis of multi-mode signals of the SASW method." *Proc., 7th Int. Conf. Soil Dynamics and Earthquake Engineering*, Chania, Crete, 259–266.
- Aouad, M. F. (1993). "Evaluation of flexible pavements and subgrades using the spectral-analysis-of-surface-waves (SASW) method." PhD thesis, Univ. of Texas at Austin, Tex.
- Buchen, P. W., and Ben-Hador, R. (1996). "Free-mode surface-wave computations." *Geophys. J. Int.*, 124, 869–887.
- Dunkin, J. W. (1965). "Computation of modal solutions in layered, elastic media at high frequencies." *Bull. Seismol. Soc. Am.*, 55(2), 335–358.
- Ganji, V., Gucunski, N., and Nazarian, S. (1998). "Automated inversion procedure for spectral analysis of surface waves." *J. Geotech. Eng.*, 124(8), 757–770.
- Graff, K. E. (1975). *Wave motion in elastic solids*, Oxford University Press, London.
- Gucunski, N., Abdallah, I. N., and Nazarian, S. (2000). "ANN backcalculation of pavement profiles from the SASW test." *Pavement subgrade unbound materials, and nondestructive testing*, Geotechnical Special Publication, ASCE, New York, No. 98, 31–50.
- Gucunski, N., and Woods, R. D. (1992). "Numerical simulation of the SASW test." *Soil Dyn. Earthquake Eng.*, 11(4), 213–227.
- Haskell, N. A. (1953). "The dispersion of surface waves on multilayered media." *Bull. Seismol. Soc. Am.*, 43(1), 17–34.
- Heisey, J. S., Stokoe, K. H., and Meyer, A. H. (1982). "Moduli of pavement systems from spectral analysis of surface waves." *Transportation Research Record 852*, Transportation Research Board, Washington, D.C., 22–31.
- Heukelum, W., and Foster, C. R. (1960). "Dynamic testing of pavements." *J. Struct. Div.*, 86(1), 1–28.
- Hiltunen, D. R., and Woods, R. D. (1990). "Variables affecting the testing of pavements by the surface wave method." *Transportation Research Record 1260*, Transportation Research Board, Washington, D.C., 42–52.
- Itasca consulting group, Inc. (2000). *Fast Lagrangian analysis of continua, version 4.0*. ICG, Minneapolis.
- Jones, R. (1955). "A vibration method for measuring the thickness of concrete road slabs in situ." *Mag. Concrete Res.*, 7(20), 97–102.
- Jones, R. (1962). "Surface wave technique for measuring the elastic properties and thickness of roads: Theoretical development." *Br. J. Appl. Phys.*, 13, 21–29.
- Jones, R., and Thrower, E. N. (1965). "An analysis of waves in a two-layer composite plate and its application to surface wave propagation experiments on roads." *J. Sound Vib.*, 2(3), 328–335.
- Kausel, E., and Roesset, J. M. (1981). "Stiffness matrices for layered soils." *Bull. Seismol. Soc. Am.*, 71, 1743–1761.
- Kuhlemeyer, R. L., and Lysmer, J. (1973). "Finite element method accuracy for wave propagation problems." *J. Soil Mech. Found. Div.*, 99(5), 421–427.
- Lamb, H. (1917). "On waves in an elastic plate." *Proc. R. Soc. London*, 93, 114–128.
- Lowe, M. J. S. (1995). "Matrix techniques for modeling ultrasonic waves in multilayered media." *IEEE Trans. Ultrason. Ferroelectr. Freq. Control*, 42(4), 525–542.
- Martincek, G. (1994). *Dynamics of pavement structures*, E&FN Spon and Ister Science Press, Bratislava, Slovak Republic.
- Nazarian, S. (1984). "In situ determination of soil deposits and pavement systems by spectral analysis of surface waves method." PhD thesis, Univ. of Texas at Austin, Tex.
- Nazarian, S., Yuan, D., and Tandon, V. (1999). "Structural Field Testing of Flexible Pavement Layers with Seismic Methods for Quality Control." *Transportation Research Record 1654*, Transportation Research Board, Washington, D.C., 50–60.
- Park, C. B., Miller, R. D., and Xia, J. (1998). "Imaging dispersion curves of surface waves on multi-channel records." *Technical Program with biographies, SEG, 68th Annual Meeting*, New Orleans, Expanded Abstract, Society of Exploration Geophysicists, 1377–1380.
- Park, C. B., Miller, R. D., and Xia, J. (1999). "Multichannel analysis of surface waves." *Geophysics*, 64, 800–808.
- Park, C. B., Miller, R. D., and Xia, J. (2001). "Offset and resolution of dispersion curve in multichannel analysis of surface waves (MASW)." *Proc. Symp. on the Application of Geophysics and Engineering and Environmental Problems (SAGEEP 2001)*, Environmental and Engineering Geophysical Society, Annual Meeting, Denver, SSM4.
- Park, C. B., Ryden, N., Miller, R. D., and Ulriksen, P. (2002). "Time break correction in multichannel simulation with one receiver (MSOR)." *Proc., Symp. on the Application of Geophysics to Engineering and Environmental Problems (SAGEEP 2002)*, Environmental and

- Engineering Geophysical Society, Annual Meeting, Las Vegas, 12SE17.
- Rix, G. J., Stokoe, K. H., and Roesset, J. M. (1991). "Experimental study of factors affecting the spectral-analysis-of-surface-waves method." *Research Rep. 1123-5*, Center for Transportation Research, The Univ. of Texas at Austin, Austin, Tex.
- Ryden, N. (1999). "SASW as a tool for non destructive testing of pavements." MSc thesis, Univ. of Lund, Sweden.
- Ryden, N., Ulriksen, P., Park, C. B., and Miller, R. D. (2002). "Portable seismic acquisition system (PSAS) for pavement MASW." *Proc., Symp. on the Application of Geophysics to Engineering and Environmental Problems (SAGEEP 2002)*, Environmental and Engineering Geophysical Society, Annual Meeting, Las Vegas, 13IDA7.
- Ryden, N., Ulriksen, P., Park, C. B., Miller, R. D., Xia, J., and Ivanov, J. (2001). "High frequency MASW for non-destructive testing of pavements-accelerometer approach." *Proc., Symp. on the Application of Geophysics to Engineering and Environmental Problems (SAGEEP 2001)*, Environmental and Engineering Geophysical Society, Annual Meeting, Denver, RBA-5.
- Sanchez-Salinero, I., Roesset, J. M., Shao, K. Y., Stokoe, K. H., and Rix, G. J. (1987). "Analytical evaluation of variables affecting surface wave testing of pavements." *Transportation Research Record 1136*, Transportation Research Board, Washington, D.C., 86–95.
- Stokoe, K. H., Wright, G. W., James, A. B., and Jose, M. R. (1994). "Characterization of geotechnical sites by SASW method, in Geophysical characterization of sites." ISSMFE Technical Committee #10, edited by R. D. Woods, Oxford Publishers, New Delhi, India.
- Thomson, W. T. (1950). "Transmission of elastic waves through a stratified solid medium." *J. Appl. Phys.*, 21(1), 89–93.
- Thrower, E. N. (1965). "The computation of the dispersion of elastic waves in layered media." *J. Sound Vib.*, 2(3), 210–226.
- Tokimatsu, K., Tamura, S., and Kojima, H. (1992). "Effects of multiple modes on Rayleigh wave dispersion characteristics." *J. Geotech. Eng.*, 118(10), 1529–1543.
- Valentina, S. L., Claudio, S., and Foti, S. (2002). "Multimodal interpretation of surface wave data." *Proc., 8th European Meeting of Environmental and Engineering Geophysics (EEGS-ES 2002)*, Environmental and Engineering Geophysical Society European Section, Annual Meeting Aveiro, Portugal, 21–25.
- Van der Pol, C. (1951). "Dynamic testing of road constructions." *J. Appl. Chem.*, 1 July, 281–290.
- Vidale, R. F. (1964). "The dispersion of stress waves in layered media overlaying a half space of lesser acoustic rigidity." PhD thesis, Univ. of Wisconsin, Wis.
- Xia, J., Miller, R. D., and Park, C. B. (2000). "Advantage of calculating shear-wave velocity from surface waves with higher modes." SEG 70th Annual Meeting, Calgary, Alta., Canada, Expanded Abstract, Society of Exploration Geophysicist, 1295–1298.
- Yilmaz, O. (1987). *Seismic data processing*, Society of Exploration Geophysicists.
- Yuan, D., and Nazarian, S. (1993). "Rapid determination of layer properties from surface wave method." *Transportation Research Record 1377*, Transportation Research Board, Washington, D.C., 159–166.
- Zerwer, A., Cascante, G., and Hutchinson, J. (2002). "Parameter estimation in finite element simulations of Rayleigh waves." *J. Geotech. Eng.*, 128(3), 250–261.
- Zhang, W., and Macdonald, R. A. (2001). "Models for determining permanent strains in the subgrade and the pavement functional condition." *Proc., 20th ARRB Conf., Managing Your Transport Assets*, Road Research Board, Melbourne, Australia.
- Zywicki, D. J. (1999). "Advanced signal processing methods applied to engineering analysis of seismic surface waves." PhD thesis, Georgia Institute of Technology, Atlanta.